Absolute Irradiance of the Moon for On-orbit Calibration

Thomas C. Stone and Hugh H. Kieffer

US Geological Survey, 2255 N. Gemini Dr., Flagstaff, AZ 86001, USA

ABSTRACT

The recognized need for on-orbit calibration of remote sensing imaging instruments drives the ROLO project effort to characterize the Moon for use as an absolute radiance source. For over 5 years the ground-based ROLO telescopes have acquired spatially-resolved lunar images in 23 VNIR (Moon diameter ∼500 pixels) and 9 SWIR (∼250 pixels) passbands at phase angles within ±90 degrees. A numerical model for lunar irradiance has been developed which fits hundreds of ROLO images in each band, corrected for atmospheric extinction and calibrated to absolute radiance, then integrated to irradiance. The band-coupled extinction algorithm uses absorption spectra of several gases and aerosols derived from MODTRAN to fit time-dependent component abundances to nightly observations of standard stars. The absolute radiance scale is based upon independent telescopic measurements of the star Vega. The fitting process yields uncertainties in lunar relative irradiance over small ranges of phase angle and the full range of lunar libration well under 0.5%. A larger source of uncertainty enters in the absolute solar spectral irradiance, especially in the SWIR, where solar models disagree by up to 6%. Results of ROLO model direct comparisons to spacecraft observations demonstrate the ability of the technique to track sensor responsivity drifts to sub-percent precision. Intercomparisons among instruments provide key insights into both calibration issues and the absolute scale for lunar irradiance.

Keywords: Moon, calibration, irradiance, spacecraft

1. INTRODUCTION

As space-borne remote sensing imagery becomes increasingly relied upon to monitor the terrestrial environment, the need to validate these instruments' absolute radiometric calibration assumes greater importance. Satellite instrumentation commonly suffers performance offsets in achieving orbit, and virtually all imaging systems have responsivity drifts over time. The Moon provides a suitable radiance source for on-orbit calibration: its luminous flux is in the appropriate range for nadir-viewing imagers, its spectral features are broad and relatively shallow, and it is observable from any Earth-viewing spacecraft orbit. Although the Moon's brightness is clearly variable and non-uniform, the surface reflectance properties are extremely stable,[1] making radiometric modeling feasible. Such a model can be used to establish an on-orbit calibration pathway for space-borne imaging systems.

Specifying the complex reflectance behavior of the Moon in a photometric model is simplified somewhat by integrating the lunar disk to an irradiance. The ROLO project has developed a lunar irradiance model which fits hundreds of images acquired by our automated ground-based telescope observing system,[2] corrected and calibrated to exoatmospheric radiance and summed to irradiance. The derived fit coefficients in turn generate the irradiance corresponding to a spacecraft lunar observation under the spacecraft geometric viewing conditions at standard distances. The effect of the extended limits of physical libration for on-orbit observations as compared with a fixed point on the Earth are reflected in the relative strength of the libration terms contained in the irradiance model. This points out the importance of continuing the ROLO ground-based observation program to fill out as much of the libration cycle as possible.

Spacecraft measurements of the Moon can be compared directly to the ROLO model results on an absolute scale, or the model can be used for intercomparison of measurements among many spacecraft, each with their own radiance calibration history. The ROLO project has developed a set of formal interface standards to

Further author information: (Send correspondence to T.C.S.)
e-mail: tstone@usgs.gov; voice: 928-556-7381; fax: 928-556-7014
H.H.K.: e-mail: hkieffer@usgs.gov
http://www.moon-cal.org

facilitate these comparisons; calibration teams for several instruments in the NASA EOS program (SeaWiFS, Hyperion, ALI) and the U.S. Department of Energy (MTI) are active participants. Additional instrument teams can be accommodated, although because ROLO is a NASA-funded project, support for non-NASA instruments is at the discretion of the Administration.

2. ROLO LUNAR IMAGES

The ROLO dual telescopes, located on-site at the US Geological Survey field center in Flagstaff, AZ (lat. 32° 12′ 52.9″N, lon. 111° 38′ 5.0″W, alt. 2148 m), observe the Moon and stars each month when the Moon is at phase angle within ±90°. Images are acquired in 32 passbands between 350 and 2500 nm, 23 at VNIR wavelengths using a 512×512-pixel CCD, and 9 in SWIR with a 256×256 HgCdTe array. Seven of the VNIR filters are identical to EOS instrumentation currently on orbit, the other 16 are Nyquist pairs within standard astronomical bands (for color corrections for stars with different temperatures). Lunar observations are acquired at approximately half-hour intervals when the Moon is higher than 30° above the horizon. The remainder of observing time (∼75% when the Moon is accessible) is dedicated to stellar observations for atmospheric extinction determination. The extinction algorithm processes multiple observations of a subset of 190 standard stars acquired through each observing night, producing extinction coefficients which are used to correct the lunar images. The brightness difference between stars and the Moon is accommodated by inserting a neutral density filter into the optical path for lunar measurements. In 5+ years of operation, ROLO has acquired over 83000 lunar images and well in excess of 800 000 star images.

The raw lunar images are corrected for detector artifacts and normalized by exposure time to instrument response rates in Digital Numbers per unit time (DN/sec). Details of the ROLO standard data reduction procedures are found in Ref. 3. Throughout the processing steps, the acquisition sequence of filters (i.e. bands) is maintained in consolidated image cubes, sorted by (increasing) wavelength, with a single header containing band-parallel ancillary data for an entire cube. Irradiance sums are generated by integrating the full lunar disk, regardless of its illuminated fraction. A field background level (nominally near-zero radiance) is measured in an annular region surrounding each Moon image and subtracted from the irradiance sum. Both the corrected sum and background values are recorded in the image cube header, along with their respective uncertainties. The images in detector physical space are then mapped onto a 576×576-pixel grid fixed to selenographic coordinates in a modified Lambert Azimuthal Equal-area conformal projection. The extent of this "ALEX" projection covers all points on the Moon ever visible from Flagstaff.

Nightly evaluations of atmospheric extinction are derived from analysis of 7–12 selected stars which are observed repeatedly throughout the night. Other stars with varied color temperatures are observed typically twice per night to constrain the extinction fit, as the fitting process is band-coupled. The algorithm finds a least-squares solution for the abundances of absorbing species, which are allowed to vary smoothly over time. The method generally follows that of Ref. 4. Absorption spectra are generated from MODTRAN v3.7 for the "normal" atmospheric gases (N_2, O_2, CO_2, etc.), water vapor, and ozone, plus Rayleigh scattering and four aerosols. The absorber amounts can vary independently in time, but all filter bands are fitted simultaneously. The time dependence is modeled by a second-order Chebyshev polynomial. The resulting set of fit coefficients are written to an ancillary parameter file, used to generate extinction corrections for the lunar images. An additional product is exoatmospheric irradiance measurements of the observed stars; these augment a larger ROLO database and are used for periodic instrument performance assessments and stellar photometric analysis.

The absolute radiance scale is based upon measurements of the star Vega (α Lyr) directly by the ROLO telescopes and published in the astronomical literature.[5,6] Vega is one of the ROLO standard stars, regularly observed when visible in the night sky (April–September). In a dedicated reprocessing of all ROLO observations of Vega through March 2001, the atmospheric extinction model was applied iteratively to cull lower quality measurements and converge on the exoatmospheric irradiance expressed as instrument response rates (in DN/sec) for the ROLO bands. A stellar model atmosphere for Vega (`veg090250000p.asc49`[7,8]) was scaled to the absolute photometric measurements of Refs. 5 and 6, then convolved with the ROLO spectral response functions to give effective photon fluxes for Vega in each band. The flux/DN rate ratio establishes the baseline for the absolute radiance scale, modified by a model for long-term degradation of the telescope optics.

Neither the atmospheric correction nor radiance calibration are applied to the ALEX-projected images, but rather parametric data are recorded in the image file headers. After every standard processing run the aggregate set of ALEX image files are parsed to build a table of selected header entries, including the irradiance sums, observational geometry and ephemerides, and the extinction and calibration factors. These are sorted by acquisition time of the individual images, producing 32-band sequences from VNIR/SWIR cube file pairs. This auxiliary parameter table forms the input database for ROLO lunar irradiance modeling.

3. LUNAR IRRADIANCE MODEL

3.1. Model Inputs – Processing

Although the ROLO model comparisons initially involve images of the Moon processed to absolute radiance and summed to irradiance, the development of model fit coefficients is done in dimensionless reflectance. The auxiliary table parameters combine to give the lunar absolute irradiance $\mathcal{I}$ at standard distance by:

$$\mathcal{I}_{\oslash} = (I_{\Sigma} \cdot C_L \cdot C_{ext}) \cdot \Omega_p \cdot f_D \tag{1}$$

where I_{Σ} is the instrument response irradiance sum, C_L is the radiance calibration factor, C_{ext} is the extinction correction, and Ω_p is the solid angle of one pixel. The correction factor to standard distance is:

$$f_D = \left(\frac{D_{\oslash}}{384400} \right)^2 \cdot D_{\odot}^2 \tag{2}$$

where $D_{\oslash}$ is the Moon–observer distance in km and $D_{\odot}$ is the Moon–Sun distance in AU. The conversion from irradiance to disk reflectance is given by:

$$\mathcal{I}_{\oslash\lambda} = A_{\oslash\lambda} \cdot \Omega_{\oslash} \cdot E_{\odot\lambda}/\pi \tag{3}$$

where $A_{\oslash}$ is the disk-equivalent albedo (full Lambert lunar disk), λ is the effective wavelength of a band, $\Omega_{\oslash}$ is the solid angle of the Moon and $E_{\odot}$ is the solar spectral irradiance, the latter two at standard distances ($\Omega_{\oslash} = 6.4236 \times 10^{-5}$ sr). This conversion involves a solar spectral irradiance model, which may have significant uncertainties in some wavelength regions; however, the direct dependence on solar model cancels to first order as long as the same model is used in going from irradiance to reflectance and back. Models which include physically-based photometric functions show an increased sensitivity to uncertainties in the solar model due to explicit dependencies on the absolute reflectance. All work thus far has ignored variation with time of the solar spectral irradiance. The variation of total solar irradiance is about 0.2%,[9] although this is considerably greater in the ultraviolet.

3.2. Lunar Disk Reflectance Model

The Moon exhibits a pronounced increase in luminosity at small phase angles, a phenomenon commonly referred to as the "opposition effect". A recent analysis[10] of Clementine images has shown the opposition effect becomes increasingly strong to phase angles as small as 0.1°, is stronger over highlands than maria, and has a slight increasing trend toward shorter wavelengths. Investigations using physically-based models to fit these observations have concluded the major cause is shadow hiding[10, 11] or shadow hiding and coherent backscatter.[12] The sample data given in Figure 1 show the opposition enhancement clearly.

Efforts to fit the extensive ROLO irradiance measurement database using physically-based models have resulted in residuals considerably larger than the scatter in the observational data. A series of iterative internal consistency checks has shown the accuracy of the ROLO measurements exceeds the capability of current physical photometric models to predict them. This is clearly an area for further work. As a consequence, the current ROLO modeling activity has focused on development of an empirical analytical expression in the primary geometric variables. The present form of the model is, for each band k:

$$\ln A_k = \sum_{i=0}^{3} a_{ik} g^i + \sum_{j=1}^{3} b_{jk} \Phi^{2j-1} + c_1\theta + c_2\phi + c_3\Phi\theta + c_4\Phi\phi + d_{1k}e^{-g/p_1} + d_{2k}e^{-g/p_2} + d_{3k}\cos((g-p_3)/p_4) \tag{4}$$

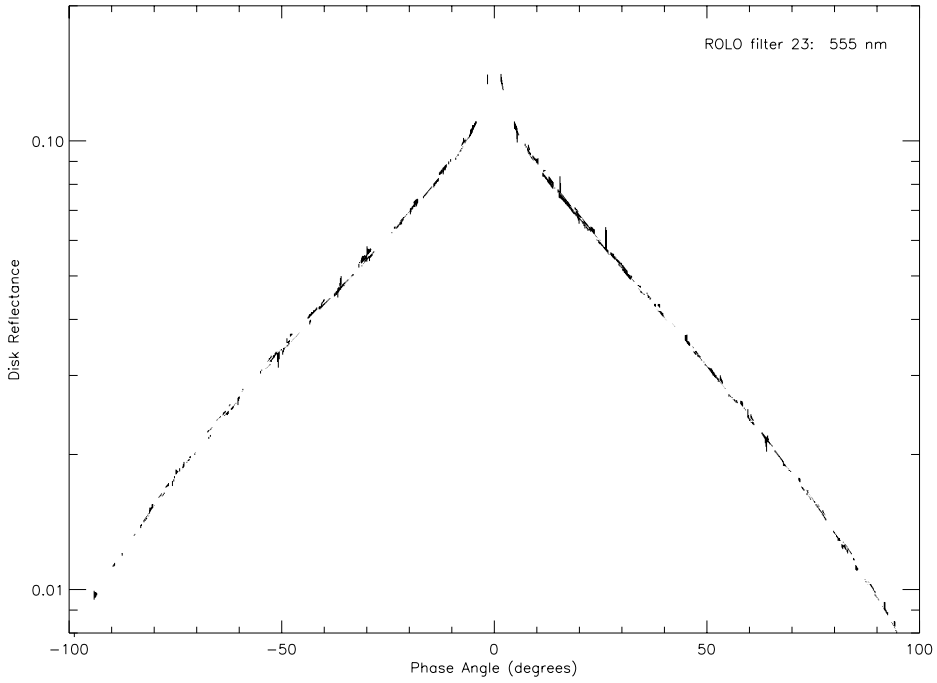

Figure 1. Disk Reflectance vs. Phase Angle. The plot symbols are (vertical) lines drawn between the ROLO data (expressed as the term $A_{\oslash}$ in Equation 3) and the corresponding model results. Indication of the sign of the difference has been lost in the image reproduction.

where A_k is the disk-equivalent reflectance, g is the absolute phase angle, Φ is the selenographic longitude of the Sun, and θ and ϕ are the selenographic latitude and longitude of the observer.

The first polynomial represents the basic photometric function dependence upon phase angle, neglecting the opposition effect. The second polynomial approximates the asymmetry of the surface of the Moon that is illuminated, primarily the distribution of maria and highlands. The c-coefficient terms account for the face of the Moon that is actually observed (topocentric libration), with a consideration of how it is illuminated. The form of the last three terms, all non-linear in g, is strictly empirical. The first two represent the opposition effect and the last one simply addresses a correlation seen in the irradiance residuals.

The ROLO data selected for fitting are constrained to $1.55^\circ < g < 97^\circ$ (the lower limit is slightly conservative, before the onset of eclipse phenomena) and the requirement that all images used be part of complete 32-filter sequences; the latter eliminates all nights preceding startup of the SWIR instrument in January 1998. Remaining data are weighted based upon nightly observing conditions. Two iterations of a least-squares fitting process were applied using the above form, except all the non-linear terms were omitted. After the first fit, data with residuals greater than 3 standard deviations of the residual average are removed. After the second fit, any point with residual >0.25 is removed. This process leaves about 1150 observations for each filter. A fitting process which handles both the linear and non-linear terms in multiple steps yields 8 coefficients which are constant over wavelength (4 for libration and the 4 opposition effect parameters) and 9 coefficients for each filter band. The mean absolute residual over the set of utilized data is 0.0096 in natural logarithm of irradiance.

A sample of ROLO image-derived data and the corresponding model-generated reflectance values is shown in Figure 1. Observed disk reflectances are generated by Equations 1 to 3. The opposition effect is readily apparent at small phase angles, as is the asymmetry between waxing and waning phases. Less discernible in this figure is the accounting for topocentric libration present in the model results, which can show up to 5% deviations from a putative smooth function of phase.

A representative set of fit coefficients, averaged over the ROLO bands, is shown in Table 1. These should not be used to calculate the lunar albedo at any wavelength; they are characteristic values generated only for demonstrating the relative importance of each term in Equation 4. The column labeled "Effect" gives the magnitude of change in $\ln A$ over the full range of variables in each term. The total effect of the libration terms is about 7%, of which about half results from the optical librations (without Φ). These magnitudes are comparable to estimates made by integrating the albedo of appropriate faces of the Moon using a digital map constructed from Clementine data.[13]

Table 1. Sample Lunar Irradiance Model Coefficients

Symbol	Term	Name	Value	Units	Effect
a_0	g^0	Constant	-1.889	–	
a_1	g^1	Phase 1	-1.627	radian^{-1}	2.811
a_2	g^2	Phase 2	0.4384	radian^{-2}	1.309
a_3	g^3	Phase 3	-0.2349	radian^{-3}	1.212
b_1	Φ^1	SunLon 1	0.04252	radian^{-1}	0.147
b_2	Φ^3	SunLon 3	0.01324	radian^{-3}	0.137
b_3	Φ^5	SunLon 5	-0.005092	radian^{-5}	0.157
c_1	θ	Libr X	0.000322	deg^{-1}	0.0052
c_2	ϕ	Libr Y	-0.001354	deg^{-1}	0.0217
c_3	$\Phi\theta$	SunLon*LibX	0.000956	deg^{-1} radian^{-1}	0.026
c_4	$\Phi\phi$	SunLon*LibY	0.000634	deg^{-1} radian^{-1}	0.017
d_1	e^{-g/p_1}	1st expon.	0.3894	–	0.264
p_1			3.98	degree	
d_2	e^{-g/p_2}	2nd expon.	-0.1477	–	0.130
p_2			12.19	degree	
d_3	$\cos((g-p_3)/p_4)$	cosine	-0.003453	–	0.004
p_3		phase	-43.48	degree	
p_4		period	18.73	degree	

3.3. Model Absolute Scale Adjustment

The reflectances produced by direct fitting of the ROLO irradiance measurements yield spectra with some sharp structure inconsistent with the broad and relatively shallow spectral reflectance features of the Moon. These possibly could be artifacts related to the solar spectral irradiance model used, or may originate with the stellar calibration method, both of which involve wavelength convolutions with the filter passbands. To better approximate the spectral properties of the Moon, the model output scale is adjusted using laboratory reflectance spectra of returned Apollo samples. A synthetic spectrum constructed of a mixture of 95% soil (Apollo 16 soil: 62231[14,15]) and 5% breccia[16] was scaled to fit the ROLO-generated spectrum for g=7°, Φ=7°, θ=0, ϕ=0. A piecewise linear interpolation method was used to generate correction factors which scale the ROLO spectrum while preserving the curvature of the laboratory spectrum. The correction spectra are shown in Figure 2; the average adjustment is about 3.5%.

4. SPACECRAFT LUNAR IRRADIANCE COMPARISONS

Comparative measurements of the absolute lunar irradiance measured by spacecraft requires a photometric model. For ROLO model comparisons, spacecraft observations are processed to radiance using the usual calibration method for the instrument, then integrating the calibrated image to an irradiance. The observation geometry and all necessary corrections (e.g. standard distances, oversampling, etc) are calculated and applied by the ROLO team. Model-generated reflectance values A_k for the particular illumination and viewing geometry are interpolated to the spacecraft wavelengths (currently linear interpolation is used), then converted

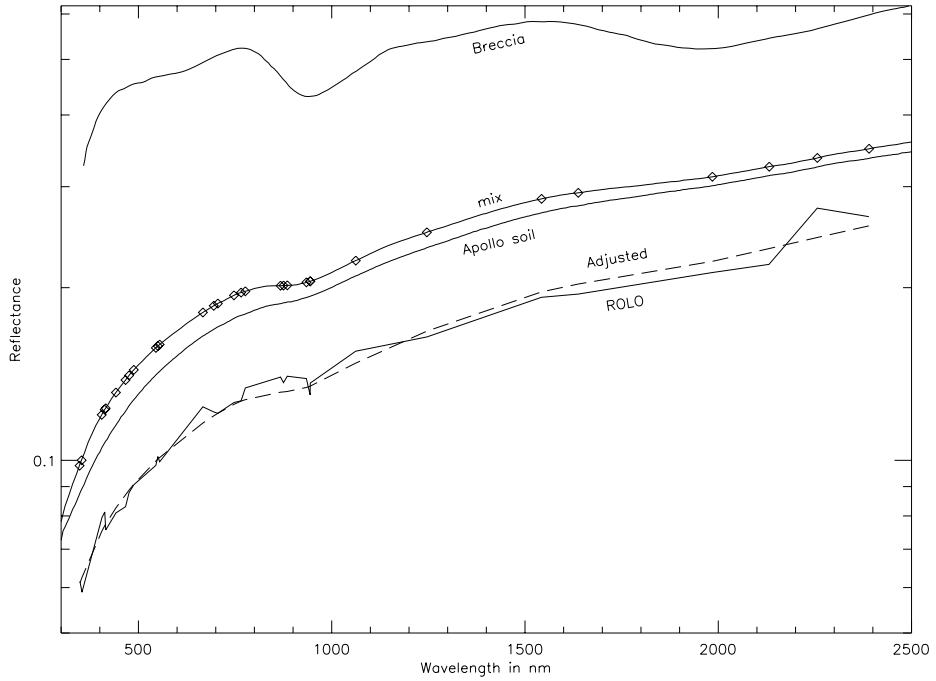

Figure 2. Lunar Reflectance Spectra. The diamonds show the effective reflectance of the soil/breccia mixture at ROLO wavelengths used to adjust the preliminary ROLO model outputs to replicate the smooth spectral properties of the lunar surface.

to irradiance via Equation 3 using the same solar spectral model with which the fit coefficients were determined. The report to the instrument teams includes the modeled absolute irradiance and the discrepancy to the spacecraft measurements, given in percent: ((spacecraft/ROLO)–1)×100%. A formal protocol for exchange of information between ROLO and spacecraft teams has been established; these can be reviewed at the ROLO website: `www.lunar-cal.org`.

The recommended spacecraft viewing geometry is a phase angle between 4° and 10°— a compromise to maximize the luminosity while avoiding strong opposition effect conditions. This configuration is achievable twice per month for several orbits, but requires a spacecraft attitude maneuver for nadir-viewing instruments. As indicated by the relative influence of model terms shown in Table 1, topocentric libration is an important parameter for accurately representing spacecraft measurements of the Moon, and should be considered in planning lunar views.

The ROLO program facilitates comparisons of absolute lunar irradiance measurements, both directly between spacecraft and the ROLO model results, and intercomparisons among different instruments. Several NASA–EOS instruments are viewing the Moon regularly, each having its own calibration scale and methodology. One goal of ROLO is to assemble this multiplicity of measurements to reassess the absolute scale for lunar irradiance. To that end, we require that instrument teams participating in the ROLO lunar calibration program furnish absolute irradiance derivations for their observations, employing their usual calibration methods.

4.1. SeaWiFS

SeaWiFS has observed the Moon almost every month for more than 4 years. The nadir-viewing satellite executes a pitch maneuver during the nightside pass of its sun-synchronous orbit, with SeaWiFS capturing the Moon as the satellite crosses the sub-lunar point on the orbit track. Observations are typically made at ∼7° phase angle, roughly evenly split between before and after Full Moon. The lunar image is small, 6×20 pixels, a potentially significant source of uncertainty in determining the down-track size, and therefore the oversampling factor.

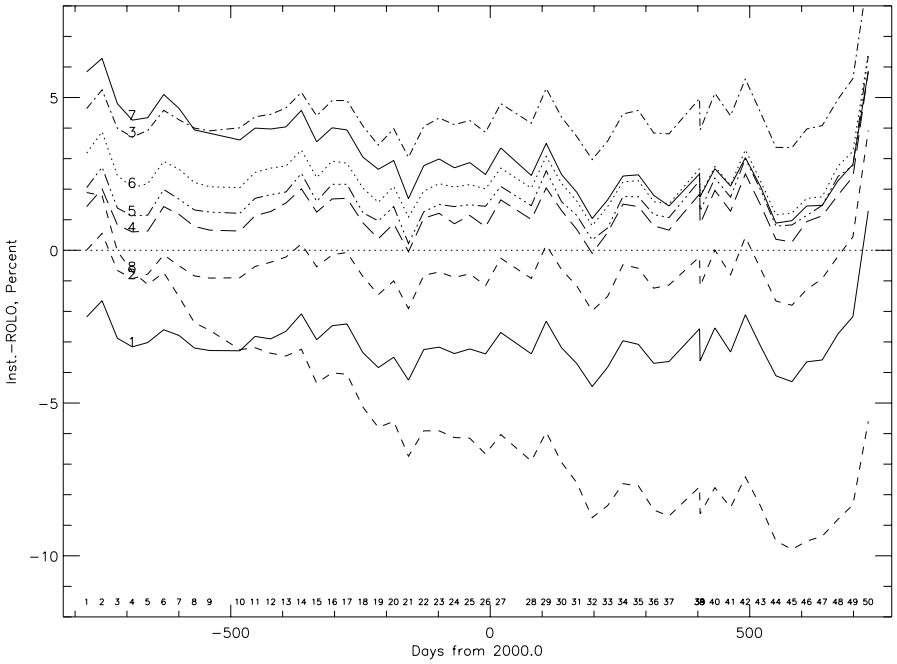

Figure 3. SeaWiFS Lunar Irradiance Comparison – Time Sequence. The observation index is shown across the bottom, SeaWiFS bands are numbered at left

Table 2. SeaWiFS Irradiance Comparison – Trends

Band	Wavelength	Average	Trend (yr^{-1})	$<$ |residual| $>$
1	412	-3.03	-0.03	0.57
2	443	-0.60	0.04	0.57
3	490	4.38	0.15	0.58
4	510	1.25	0.18	0.56
5	555	1.70	0.14	0.58
6	670	2.33	-0.04	0.58
7	765	3.03	-0.74	0.61
8	865	-5.71	-2.26	0.85

Figure 3 shows the time sequence of irradiance comparisons in each band for SeaWiFS lunar observations through December 2001, given as percent discrepancy with the ROLO model. The temporal jitter is nearly identical in all bands — within this common profile the deviations are well under 1%. Because the coefficients SeaWiFS uses for radiance calibration are constant in time, these comparisons constitute a direct measure of detector performance stability. The trends in bands 1–6 are essentially flat, while bands 7 and 8 show decreasing sensitivity with time. The temporal trends are summarized in Table 2; all analysis values are given in percent. The "Average" values are taken over the full set of lunar observations in a band; the mean absolute residuals reflect the precision of the band averages.

4.2. EO–1

EO–1 now acquires lunar observations each month at absolute phase angles $\sim 7°$, similar to SeaWiFS. The spacecraft attitude maneuver is a similar pitch to the Moon, but includes a raster scan over the lunar disk with a down-track pitch rate giving $\sim 8.5\times$ oversampling. The alignment offset between ALI and Hyperion allows

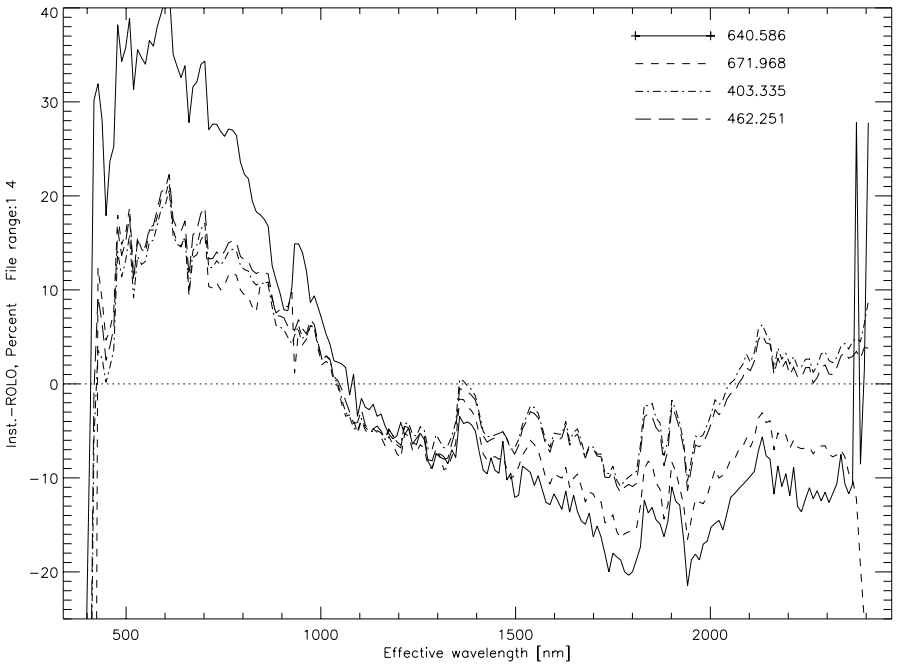

Figure 4. Hyperion Lunar Irradiance Comparison Spectra. The legend indicates the observation time in days from (year) 2000.0

only one instrument to observe the Moon at a time, therefore lunar views in each are acquired on an alternating schedule.

Hyperion's 7.5-km cross-track swath (0.623° field of regard) allows little tolerance for capturing the entire lunar disk; most observations to date have been clipped on an edge. The Hyperion images provided to ROLO have dissimilar processing histories, leading to uncertainties in their absolute radiance scales. As a consequence, the absolute scale for each date has been adjusted by an arbitrary amount to yield similar averages over wavelength in the ROLO comparisons.

Figure 4 shows irradiance model spectral comparisons for four Hyperion lunar observations, again given as percent discrepancy. The dense spectral structure observed, nearly coincident in all four spectra, is uncharacteristic of lunar reflectance, nor does it originate in the ROLO model wavelength interpolation, which is smooth. Some water vapor band features might be traced to the instrument pre-launch calibration, where problems with optical absorption in the laboratory have been identified. The significant overall color trend apparent in the day-640 plot remains unexplained.

Nine ALI lunar observations have been compared against the ROLO irradiance model, 3 before Full Moon and 6 after. All instrument image processing is conducted by the ALI team, who provide ROLO with image-based irradiance integrations (which include oversampling), the down-track angular size of the lunar image, and the time and spacecraft coordinates of the observations. Instrument spectral response parameters have been provided t ROLO for calculating band effective wavelengths for a lunar spectrum.

Preliminary comparison results for ALI are shown in Figure 5. The discrepancy excursions generally follow the Hyperion spectra, though not in all wavelength regions (e.g. band 5p). The observed temporal trends are neither strong nor monotonic; a summary is given in Table 3. **Note**: these results are derived from preliminary ALI lunar image processing, and should not be considered indicative of actual spacecraft sensor performance.

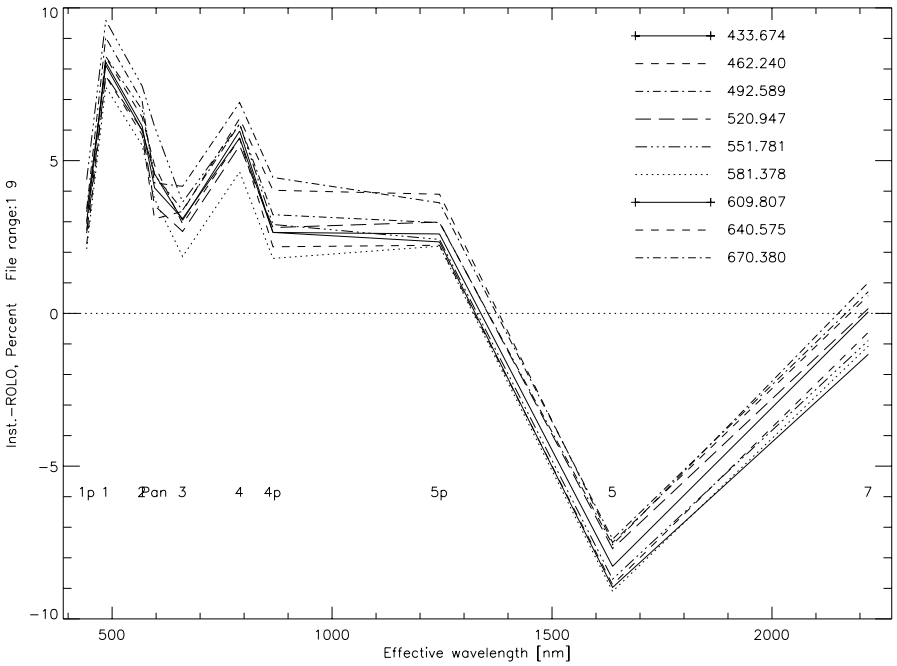

Figure 5. ALI Lunar Irradiance Comparison Spectra. The band indexes locate effective wavelengths, the legend indicates observation time in days from 2000.0

Table 3. ALI Lunar Irradiance Comparison

Band	Wavelength	Average	Trend (yr^{-1})	$<$ |residual| $>$
1p	442	3.51	-0.35	0.48
1	485	7.98	0.21	0.47
2	567	5.58	0.50	0.44
Pan	592	2.73	1.05	0.62
3	660	4.01	-0.58	0.45
4	790	7.22	-0.86	0.44
4p	865	5.40	-1.61	0.60
5p	1245	4.47	-1.10	0.46
5	1640	-7.69	-0.36	0.60
7	2225	-1.15	0.66	0.73

4.3. MTI

MTI has acquired numerous observations of the Moon, six of which were selected by the MTI team for processing for ROLO irradiance comparisons, 3 prior to and 3 following a solar exposure incident involving one of the three focal plane detector assemblies. The results of the ROLO comparisons have boosted the team's confidence in their recovery efforts following the mishap. Figure 6 shows MTI comparison spectra. Band G (1010 nm) appears to be increasing in responsivity with time; the other bands show no monotonic temporal trends. The overall scale is highly correlated among the bands; however, the MTI lunar image processing and calibration are still preliminary. At SWIR wavelengths the spectral shape appears very similar to the EO–1 results, deviating from this trend somewhat for shorter wavelengths.

The similarities among the different instruments suggest uncorrected systematic errors may exist in the ROLO data processing, or they may be indicative of problems with use of the solar spectral models in converting

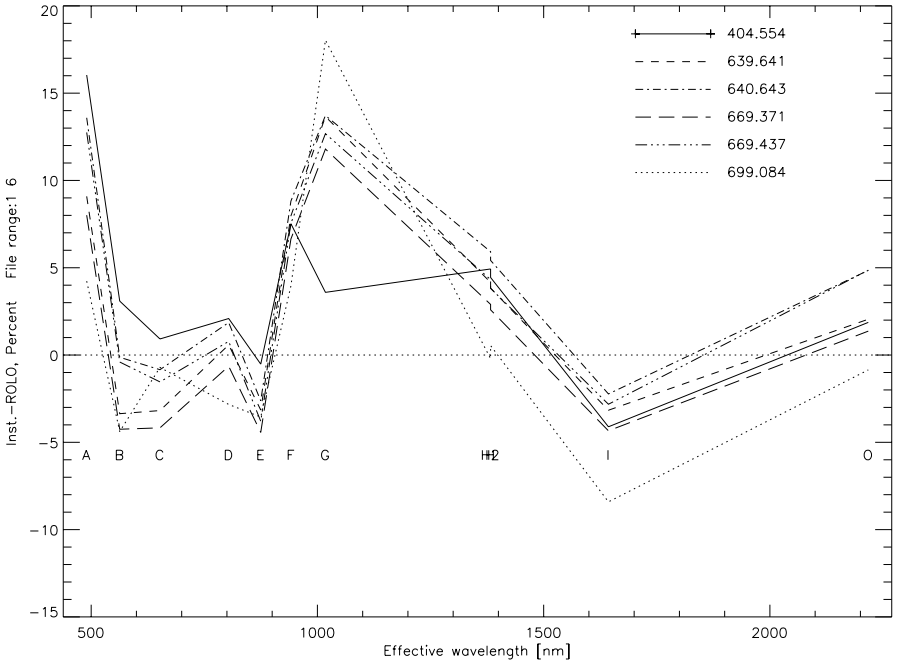

Figure 6. MTI Lunar Irradiance Comparison Spectra. The band indexes locate effective wavelengths, the legend indicates observation time in days from 2000.0

to reflectance (cf. Eqn. 3). For the ROLO irradiance work several solar models were tested, settling on the 1986 World Climate Research Program data.[17] Intercomparisons among the various spacecraft measurements may be exposing the limits of uncertainty for available solar spectral irradiance measurements.

5. CONCLUSIONS

The ROLO project has developed an empirical photometric model capable of determining the lunar irradiance for Earth-orbit viewing geometries at phase angles within $\pm 90°$. Model inputs are derived from about 37000 of the 83000+ lunar images acquired by the ROLO ground-based telescopes. Corrections for the atmosphere are developed from nightly observations of standard stars using a band-coupled multiple atmospheric component extinction algorithm. The absolute radiance scale is based upon independent measurements of the star Vega. Radiance-calibrated images integrated to irradiance quantities provide the sample data for the photometric model, expressed in terms of reflectance (i.e. disk-equivalent albedo) using a model solar irradiance spectrum. The ROLO model fit coefficients allow determination of the lunar irradiance corresponding to observations acquired by Earth-orbiting spacecraft. Model results are interpolated to spacecraft instrument wavelengths.

Much has been revealed by initial model comparisons of irradiance measurements taken by four spacecraft instruments. The spectral deviations in the direct model comparisons, as well as the observed differences between instruments, exceed the model relative errors, even when constraints on the model absolute scale are relaxed. When nulling factors are used to offset correlated temporal jitter, the comparisons can track sensor responsivity drifts to the sub-percent level, approaching 0.1% in the case of SeaWiFS. The observed discrepancies among different instruments could be indicative of the difficulty in establishing an absolute radiance calibration and maintaining it on orbit. Differences could also result from using different solar spectral models for the instrument lunar irradiance calculations. The disagreement among solar irradiance models, especially at SWIR wavelengths, points out an area of research in need of further development.

A protocol by which spacecraft teams interface with the ROLO lunar comparison program has been established, in the form of standard formats for instrument and observational data exchange. Intercomparisons

among different instruments help advance the ROLO effort toward specifying the absolute lunar irradiance scale at the percent or sub-percent level. Spectral measurements, such as Hyperion's, can provide extremely valuable input to this endeavor.

ACKNOWLEDGMENTS

The authors thank the calibration teams for SeaWiFS, Hyperion, ALI, and MTI for use of their lunar irradiance measurements in this paper. The ROLO project is supported by NASA Goddard Space Flight Center under contract S-41359-F.

REFERENCES

1. H. H. Kieffer, "Photometric Stability of the Lunar Surface", *Icarus* **130**, pp. 323–327, 1997
2. H. H. Kieffer and R. L. Wildey, "Establishing the Moon as a Spectral Radiance Standard," *J. Atmos. and Ocn. Tech.* **13**, pp. 360–375, 1996
3. T. C. Stone, H. H. Kieffer and J. M. Anderson, "Status of Use of Lunar Irradiance for On-orbit Calibration", *Proc. SPIE* **4483**, pp. 165-175, 2002
4. G. W. Lockwood and D. T. Thompson, "Atmospheric Extinction: The Ordinary and Volcanically Induced Variations, 1972–1985," *Astron. J.* **92**, pp. 976–985, 1986
5. D. S. Hayes, "Stellar Absolute Fluxes and Energy Distributions from 0.32 to 4.0 microns," in *Calibration of Fundamental Stellar Quantities; Proceedings of the Symposium, Como, Italy, May 24–29, 1984*, pp. 225–252, D. Reidel Publishing Co. (Dordrecht), 1985
6. D. W. Strecker, E. F. Erickson, and F. C. Witteborn, "Airborne stellar spectrophotometry from 1.2 to 5.5 microns — absolute calibration and spectra of stars earlier than M3," *Astrophys. J. Supp.* **41**, pp. 501–512, 1979
7. `HTTP://CFAKU5.HARVARD.EDU/stars/VEGA/`
8. F. Castelli and R. L. Kurucz, "Model atmospheres for Vega," *Astron. Astrophys.* **281**, pp. 817–832, 1994
9. C. Frohlich, "Observations of irradiance variations," *Space Sci. Rev.* **94**, pp. 15–24, 2000
10. B. J. Buratti and J. K. Hillier and M. Wang, "The Lunar Opposition Surge: Observations by Clementine," *Icarus* **124**, 2, pp. 490–499, 1996
11. J. K. Hillier, "Shadow-Hiding Opposition Surge for a Two-Layer Surface," *Icarus* **72**, pp. 15–27, 1997
12. B. W. Hapke and R. Nelson and W. Smythe, "The Opposition Effect on the Moon: Coherent Backscatter and Shadow Hiding," *Icarus* **133**, pp. 89–97, 2000
13. H. H. Kieffer and J. A. Anderson, "Use of the Moon for spacecraft calibration over 350–2500 nm," *Proc. SPIE* **3438**, pp. 325–335, 1998
14. `http://www.planetary.brown.edu/pds/AP62231.html`
15. C. M. Pieters, "The Moon as a Spectral Calibration Standard Enabled by Lunar Samples: The Clementine Example," in *Workshop on New Views of the Moon II: Understanding the Moon Through the Integration of Diverse Datasets*, Flagstaff, AZ., Lunar and Planetary Instit. Contrib., sept. 1999, pp. 47–48
16. C. M. Pieters and J. F. Mustard, "Exploration of crustal/mantle material for the Earth and Moon using reflectance spectroscopy," *Rem. Sens. Environ* **24**, pp. 151–178, 1988
17. C. Wehrli, "Spectral Solar irradiance data," in *World Climate Research Program (WCRP) Publication Series No. 7, WMO ITD-No. 149*, pp 119–126, 1986